REPORT NO. 826

A METHOD FOR DETERMINING THE CAMBER AND TWIST OF A SURFACE TO SUPPORT A GIVEN DISTRIBUTION OF LIFT, WITH APPLICATIONS TO THE LOAD OVER A SWEPTBACK WING

By Doris Cohen

SUMMARY

A graphical method is described for finding the shape (camber and twist) of an airfoil having an arbitrary distribution of lift. The method consists in replacing the lifting surface and its wake with an equivalent arrangement of vortices and in finding the associated vertical velocities. By a division of the vortex pattern into circular strips concentric about the downwash point instead of into the usual rectangular strips, the lifting surface is reduced for each downwash point to an equivalent loaded line for which the induced velocity is readily computed. The ratio of the vertical velocity to the stream velocity is the slope of the surface in the free-stream direction.

In order to illustrate the application of the method, the shape of the wing consistent with the pressure distribution given by the two-dimensional theories has been found for three wings: an elliptical wing of aspect ratio 6 with 30° sweepback is treated in some detail; final results are presented for two unswept elliptical wings of aspect ratios 6 and 3, respectively, to show the degree of approximation involved in the use of the two-dimensional theories for three-dimensional flow. It is concluded that the two-dimensional theories are adequate over most of the span of a straight wing but that the more exact treatment is necessary in the tip regions or if the wing is swept.

Application of the method to solve the reverse problem—finding the lift distribution over a given surface—is also illustrated. The load over an uncambered, untwisted, elliptical wing with 30° sweepback has been calculated by successive corrections of the assumed vortex distribution. The result indicates a 14-percent loss in total lift due to the introduction of sweepback with the greatest loss taking place at the center of the span.

INTRODUCTION

Because of the effect that the pressure gradients over the surface of a wing have on the drag, it would be of considerable advantage to be able to specify the camber and the twist of a wing that would produce a desired distribution of lift. Present methods of airfoil design depend on two-dimensional-flow theories, which treat the spanwise and chordwise components of the flow independently. Although a theoretical treatment of three-dimensional flow is given by Prandtl (reference 1) and calculations have been made for special cases (references 2 and 3), no practical procedure for the arbitrary lifting surface is indicated.

In the present paper, a method is described whereby the camber and the twist of a surface of arbitrary plan form may be determined so as to support a specified distribution of lift. For this method, the lifting surface and its wake are replaced by a distribution of vortices in a plane. The vertical velocity induced at any point on the surface by the vortex system defines the slope of the surface at that point. Thus, the problem becomes the determination of the induced velocities. A method is presented for determining these velocities which, by employing chiefly graphical means, eliminates the difficult integrations that have limited previous work.

The substitution of a plane vortex sheet for the lifting surface is analogous to the standard procedure of the two-dimensional thin-wing-section theory (see, for example, reference 4, p. 87), in which the flow about a thin, cambered section is approximated by an arrangement of vortices along the chord line. Inasmuch as the induced normal velocities are assumed to be substantially the same at the chord line and at the airfoil, the ratio of these velocities to the free-stream velocity gives the slope of the camber line. In three-dimensional flow a reference plane is assumed, so situated that the airfoil may be considered to be a slight deviation from it. Upon this plane the plan form and the pressure distribution of the surface are projected. As in two-dimensional treatments, the slope is calculated in the free-stream direction.

The substitution of a vortex sheet for a lifting surface is discussed at some length by Von Kármán (reference 5, p. 15). In the application of the method, however, the vortices are generally assumed to have a rectilinear distribution. Even with this limitation, the evaluation of the integrals involved in finding the induced velocities presents considerable difficulty. (See ch. IV, sec. 15, of reference 5, where the formulas are developed for a rectangular wing.) The integration is greatly simplified by the introduction of polar coordinates so chosen that the elements of integration are circular strips concentric about the point at which the downwash is to be found. Application of this method is not restricted to any particular arrangement of vortices or to any specific form of the surface.

Although the procedure described is for the determination of the surface that will fit a required pressure distribution, it may also be adapted to effect the reverse analysis, that is, to find the pressure distribution over an arbitrary surface. Such an application of the method is made to find the pressure distribution over a flat wing of elliptical plan form swept back 30° at the 50-percent-chord line.

DETERMINATION OF THE VORTEX PATTERN FROM THE PRESSURE DISTRIBUTION

The vortex pattern is obtained by integrating the chordwise pressure distribution back from the leading edge at several stations along the span. The circulation or vortex strength Γ will be shown to be proportional to this integral; the lines connecting the points where the values of the integral are equal therefore define the vortex lines.

In figure 1, a distribution of lift is arbitrarily specified for a tapered wing in straight flight. The corresponding vortex lines are drawn on the plan form of the wing and in the wake in figure 2 to show a typical vortex pattern.

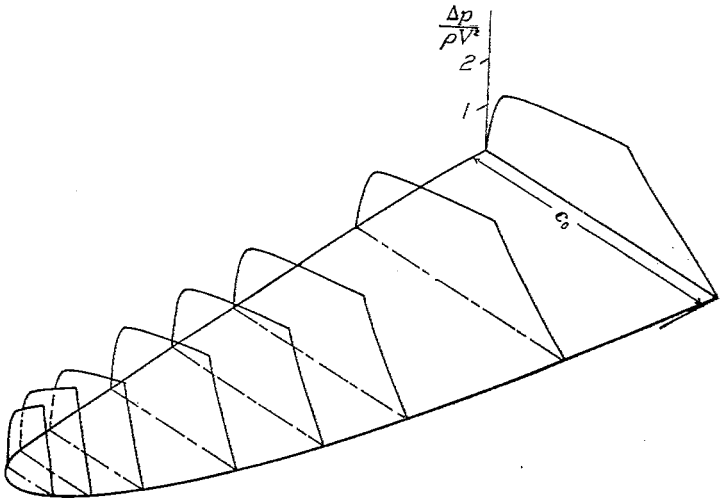

FIGURE 1.—An arbitrary distribution of lift assumed for a tapered wing in straight flight, from which the vortex lines of figure 2 were derived.

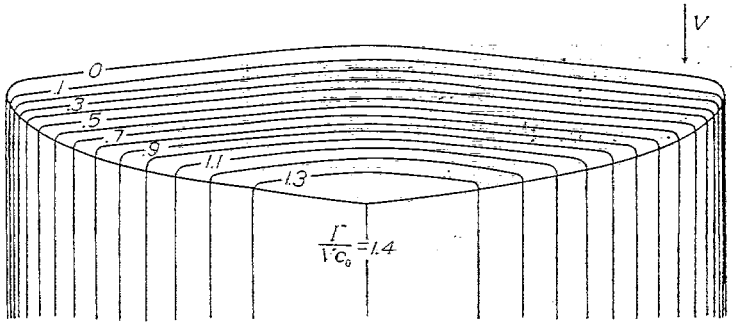

FIGURE 2.—Contour lines of circulation function, or vortex pattern, obtained by integrating the pressure distribution of figure 1.

The demonstration of the relation between the pressure distribution and the vortex pattern is given in the following paragraphs.

In the replacement of a lifting surface by a vortex sheet, the assumption is made that the pressure increments due to the presence of the airfoil in the stream are equal and opposite on the upper and lower surfaces, as would be true in the case of a thin plate at a small angle of attack. The substitution is still admissible in the calculation of lift when the thickness is not negligible, because the difference between the velocities on the upper and lower surfaces at any position and not the magnitude of each increment determines the lift at that point.

Thus, let $\Delta\mathbf{V}_u$ and $\Delta\mathbf{V}_l$ represent for any point the local velocity increments on the upper and the lower surfaces due to the plate or to the vortices that are equivalent to it; let u_u and u_l be the magnitude of their components in the direction of the free-stream velocity $\mathbf{V}$; let v_u and v_l be the components normal to $\mathbf{V}$ in the plane of the wing; and let w_u and w_l be the components normal to the wing. Then the pressure on the surfaces would be, if ρ is the air density,

$$p_u=\frac{1}{2}\rho\left|\mathbf{V}+\Delta\mathbf{V}_u\right|^2$$

$$=\frac{1}{2}\rho[(V+u_u)^2+v_u^2+w_u^2]$$

$$=\frac{1}{2}\rho(V^2+2Vu_u+u_u^2+v_u^2+w_u^2)$$

If second-order effects are neglected, this expression reduces to

$$p_u=\frac{1}{2}\rho(V^2+2Vu_u)$$

Similarly,

$$p_l=\frac{1}{2}\rho(V^2+2Vu_l)$$

The resulting lift per unit area is then the difference in pressure, or

$$\Delta p=\frac{1}{2}\rho(2V)(u_u-u_l) \tag{1}$$

The derivation of the equivalent vortex pattern follows directly from equation (1). If $d_s\Gamma$ represents the element of circulation around a small length ds, parallel to $\mathbf{V}$, over which the velocities u_u and u_l may be considered constant, the following relation holds:

$$d_s\Gamma=(u_u-u_l)ds \tag{2}$$

from which equation (1) may be rewritten

$$\Delta p=\rho V\frac{\partial\Gamma}{\partial s} \tag{3}$$

Thus, the lift at every point is proportional to $\frac{\partial\Gamma}{\partial s}$, or the cross-stream component of the vorticity. Consider now a narrow strip of varying width just behind the leading edge of the vortex sheet, such that $\int\Delta p\,ds$ is constant along the strip. Such a strip would represent a vortex element of strength $\int\Delta p\,ds$. A second vortex element could be defined in the same way to lie just behind the first. From equation (3), however,

$$\frac{1}{\rho V}\int\Delta p\,ds=\Gamma \tag{4}$$

Equation (4) defines the function Γ for any point on the lifting surface as the total circulation ahead of the point.[1] Thus, the boundaries of the vortex element are lines of equal Γ.

[1] The function Γ is numerically equal to the difference in velocity potential between the surfaces, for, at any point, $u_u=\frac{\partial\phi_u}{\partial s}$ and $u_l=\frac{\partial\phi_l}{\partial s}$, where ϕ_u and ϕ_l are the potential functions over the upper and lower surfaces of the airfoil, respectively. From equation (2),

$$\frac{\partial\Gamma}{\partial s}=\frac{\partial\phi_u}{\partial s}-\frac{\partial\phi_l}{\partial s}$$

or

$$\Gamma=\phi_u-\phi_l$$

If the vortex elements are reduced in size and increased in number to form a continuous vortex sheet, their pattern is indicated, as in figure 2, by the contour lines of the function Γ. In order to satisfy the Kutta condition that there be no pressure difference across the trailing edge, these lines must leave the wing parallel to the stream velocity, as shown by equation (3). They then follow the streamlines down the wake. The drawing of these contour lines from the integral of the pressure distribution is the first step of the procedure for finding the camber and the twist of the lifting surface.

DETERMINATION OF THE INDUCED VERTICAL VELOCITIES

The induced vertical velocity at any point of the plane is obtained by integrating the Biot-Savart equation over the entire vortex pattern just described. The resulting double integration is reduced to a single integral by a relatively simple graphical procedure if a system of polar coordinates having its origin at the point is employed.

Let it be required to find the downwash w at a point P of the vortex pattern just described. Consider a small sector of the plane included between two radii from P, the angle between the radii being $d\psi$ (fig. 3). At any distance r from P,

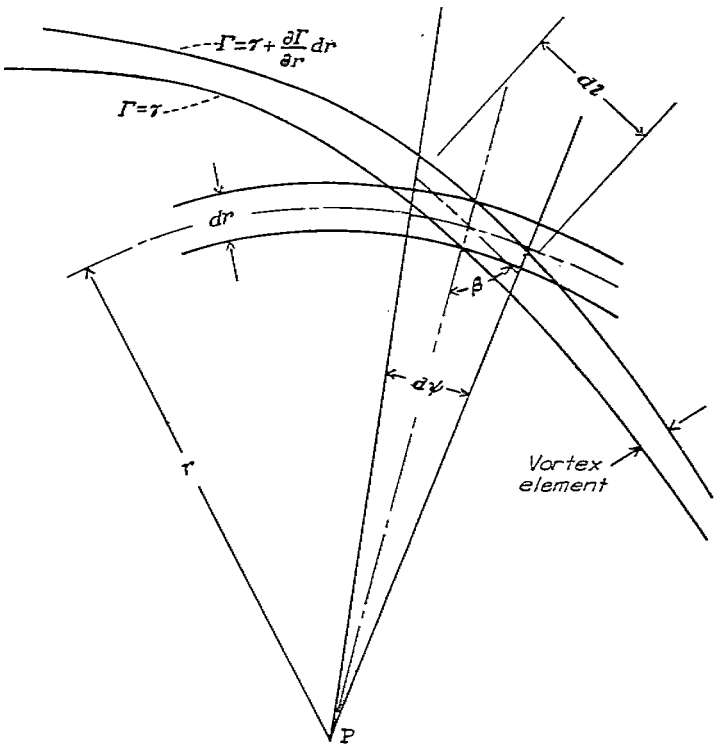

FIGURE 3.—Diagram for derivation of downwash formula $dw=-\frac{1}{4\pi r}\frac{\partial\Gamma}{\partial r}\,dr\,d\psi$.

the radii will cut off a small length dl of a certain vortex element. If the width of the element in the radial direction is dr, the strength of the vortex element is $\frac{\partial\Gamma}{\partial r}dr$. Then, by Biot-Savart's rule, the downwash at P due to the small length of vortex will be

$$dw=-\frac{1}{4\pi}\frac{1}{r^2}\frac{\partial\Gamma}{\partial r}\,dr\,dl\sin\beta \tag{5}$$

where β is the angle between the vortex element and the radius. The length $dl\sin\beta$ is the projection of dl on the circumference of the circle of radius r around P, so that

$$dl\sin\beta=r\,d\psi$$

and

$$dw=-\frac{1}{4\pi r}\frac{\partial\Gamma}{\partial r}\,dr\,d\psi \tag{6}$$

The total downwash at P would be obtained by integrating equation (6) over $0\leqq r\to\infty$ and through 360° of ψ. Thus,

$$w=\int_0^\infty\int_0^{2\pi}-\frac{1}{4\pi r}\frac{\partial\Gamma}{\partial r}\,d\psi\,dr \tag{7}$$

In order to evaluate the double integral of equation (7), the relation (Liebniz's rule)

$$\int_0^{2\pi}\frac{\partial\Gamma}{\partial r}\,d\psi=\frac{d}{dr}\int_0^{2\pi}\Gamma\,d\psi \tag{8}$$

is used to reduce the first integration to a graphical procedure.

The first step in evaluating w is to draw on the vortex pattern circles of various radii about P. Around any one circle (see fig. 4) the function Γ will take on values indicated by the

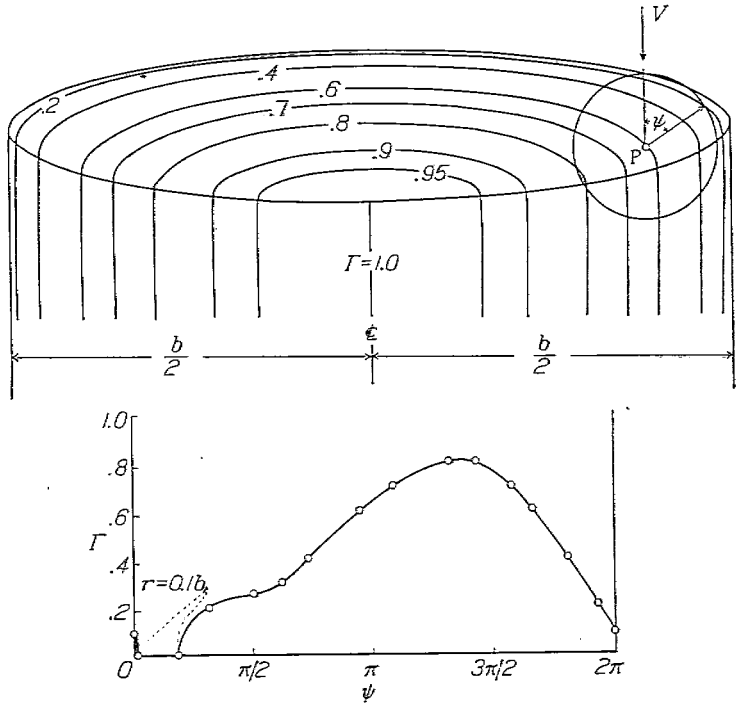

FIGURE 4.—Variation of Γ around circle, plotted against ψ from intersections of the circle with the contour lines. Additional points at $\psi=0$ and at $\psi=\frac{\pi}{2}$ are computed.

intersections of the circle with the contour lines of Γ. If these values of Γ are plotted against the angle ψ — measured, let us say, from the free-stream direction — graphical integration will give $\int_0^{2\pi}\Gamma\,d\psi$ for each circle. It is somewhat more convenient to plot Γ against $\psi/2\pi$. Then the integral will be the average value of Γ around the circle, designated in the usual way by

$$\overline{\Gamma}=\int_0^{2\pi}\frac{\Gamma}{2\pi}\,d\psi \tag{9}$$

Then $\overline{\Gamma}$ is a function of r. (See fig. 5.) From equation (8),

$$\int_0^{2\pi}\frac{\partial\Gamma}{\partial r}\,d\psi=2\pi\frac{d\overline{\Gamma}}{dr} \tag{10}$$

so that

$$w=-\int_0^\infty\frac{1}{2r}\frac{d\overline{\Gamma}}{dr}\,dr \tag{11}$$

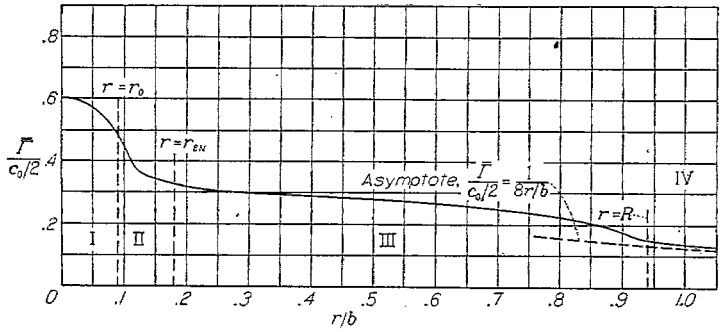

FIGURE 5.—Typical curve for $\bar{\Gamma}$ (r). (Curve for point P of fig. 4.)

For the evaluation of equation (11), first plot $\bar{\Gamma}$ against r, as in figure 5. The curve will approach an asymptote, which is readily found from the expression for the load curve across the wake. Thus, when r is large, $d\psi=\frac{dy}{r}$ and equation (9) reduces to

$$\bar{\Gamma}=\frac{1}{2\pi r}\int_{-b/2}^{b/2}\Gamma(y)\,dy \tag{12}$$

where y is the spanwise dimension and $b/2$ is the semispan of the wing. If the area under the load curve across the wake is Λ, then for very large values of r

$$\bar{\Gamma}=\frac{\Lambda}{2\pi r} \tag{13}$$

The plot of $\bar{\Gamma}(r)$ should be carried out to a value of r such that the curve approaches this asymptote within the accuracy of the work.

The load curve of figure 5 is a typical one. The following method has been found particularly suited to the determination of the downwash at the origin of such a curve. The first section of the curve (designated by I), starting with zero slope, is approximated up to the inflection point, or to a point r_0 somewhat ahead of it, by an expression of the form $\bar{\Gamma}=a_0-a_2r^2-a_4r^4$. Additional terms might be used but are generally not necessary. The downwash due to a curve of the general form

$$\bar{\Gamma}=a_0-a_nr^n\ (n>1)$$

at $r=0$ is given by

$$w=-\frac{a_n}{2}\frac{n}{n-1}\left(r_B{}^{n-1}-r_A{}^{n-1}\right)$$

where r_A and r_B are the end values of r for the interval over which the curve extends. The downwash contributed by the first section of the load $\bar{\Gamma}=a_0-a_2r^2-a_4r^4$ is therefore

$$w(\mathrm{I})=a_2r_0+\frac{2}{3}a_4r_0{}^3 \tag{14}$$

The part of the curve immediately following $r=r_0$ has a critical effect on the value of the downwash, at the same time being usually too irregular to be approximated for any distance by a simple algebraic expression. It is therefore advisable to proceed as in numerical integration, dividing the curve into a finite number of small sections and considering each section of the curve to have a simple mathematical expression. Because the effectiveness of the variation of load depends on its closeness to the downwash point, the intervals are taken in geometric rather than arithmetic progression. Thus, the abscissas are r_0, kr_0, k^2r_0, . . . etc., where the ratio k is a number, usually between 1 and 2, determined by the size of the intervals required for accurate representation of the curve immediately following r_0. The usual procedure now would be to assume the curve to be a straight line over each small interval; but when the curvature is largely in one direction, as it is in these curves, this assumption introduces a small but cumulative error, which may amount to 10 percent or more in the total. The following method, which fits the curve with a succession of parabolas, is found to give very good accuracy with no increase in computation. The method is best presented in tabular form:

Computation of w

n	$r_{2n}=k^{2n}r_0$	$r_{2n+1}=kr_{2n}$	$\bar{\Gamma}$	$\Delta\bar{\Gamma}_{2n}$	$\Delta\bar{\Gamma}_{2n+1}$	$\frac{\Delta\bar{\Gamma}_{2n}}{r_{2n}}$	$\frac{\Delta\bar{\Gamma}_{2n+1}}{r_{2n}}$
	r_0		$\bar{\Gamma}_0$				
				$\bar{\Gamma}_1-\bar{\Gamma}_0$		$\frac{\Delta\bar{\Gamma}_0}{r_0}$	
0		r_1	$\bar{\Gamma}_1$				
					$\bar{\Gamma}_2-\bar{\Gamma}_1$		$\frac{\Delta\bar{\Gamma}_1}{r_0}$
	r_2		$\bar{\Gamma}_2$				
				$\bar{\Gamma}_3-\bar{\Gamma}_2$		$\frac{\Delta\bar{\Gamma}_2}{r_2}$	
1		r_3	$\bar{\Gamma}_3$				
					$\bar{\Gamma}_4-\bar{\Gamma}_3$		$\frac{\Delta\bar{\Gamma}_3}{r_2}$
	r_4		$\bar{\Gamma}_4$				
				$\bar{\Gamma}_5-\bar{\Gamma}_4$		$\frac{\Delta\bar{\Gamma}_4}{r_4}$	
2		r_5	$\bar{\Gamma}_5$				
					$\bar{\Gamma}_6-\bar{\Gamma}_5$		$\frac{\Delta\bar{\Gamma}_5}{r_4}$
	r_6		$\bar{\Gamma}_6$				
. . .	. . .	. . .	. . .	. . .	. . .	. . .	. . .
				$\bar{\Gamma}_{2N-1}-\bar{\Gamma}_{2N-2}$		$\frac{\Delta\bar{\Gamma}_{2N-2}}{r_{2N-2}}$	
$N-1$		r_{2N-1}	$\bar{\Gamma}_{2N-1}$				
					$\bar{\Gamma}_{2N}-\bar{\Gamma}_{2N-1}$		$\frac{\Delta\bar{\Gamma}_{2N-1}}{r_{2N-2}}$
	r_{2N}		$\bar{\Gamma}_{2N}$				

$K_0=k\left(k\frac{\log k}{k-1}-1\right)$

$K_1=1-\frac{\log k}{k-1}$

Totals: $\sum_{n=0}^{N-1}\frac{\Delta\bar{\Gamma}_{2n}}{r_{2n}}$ $\sum_{n=0}^{N-1}\frac{\Delta\bar{\Gamma}_{2n+1}}{r_{2n}}$

$$w=\frac{-1}{k(k-1)}\left(K_0\sum\frac{\Delta\bar{\Gamma}_{2n}}{r_{2n}}+K_1\sum\frac{\Delta\bar{\Gamma}_{2n+1}}{r_{2n}}\right)$$

In the following table are given the constants K_0, K_1, and $\frac{1}{k(k-1)}$ for several convenient values of k. Since the choice of k is not critical, the values included should serve without interpolation.

k	K_0	K_1	$\frac{1}{k(k-1)}$
1.02	0.01000	0.01000	49.02
1.05	.02582	.02420	19.04
1.07	.03667	.03340	13.35
1.10	.05325	.04600	9.091
1.15	.08222	.06827	5.797
1.20	.1127	.08840	4.167
1.25	.1446	.1074	3.200
1.30	.1780	.1255	2.564
1.50	.3246	.1891	1.333

The value of the ratio k that will give sufficiently small increments of r where the slope is large will probably be found to be smaller than necessary after the curve has become more regular and the distance from the origin larger. The computations may be interrupted here and the downwash w(II) contributed by the second section may be calculated. Then, using the last abscissa r_{2V} as a new starting point and a larger value of k, compute in the same way the downwash w(III) due to the remainder of the curve to a point where the difference between the curve and its asymptote is negligible.

For the portion of the curve extending to infinity (section IV of fig. 5), the previously determined asymptote is used and the downwash found analytically. Thus, from a large value R of r out to infinity,

$$w(\mathrm{IV}) = -\frac{1}{2}\int_R^\infty \frac{1}{r}\frac{d\bar{\Gamma}}{dr}\,dr$$

from equation (10); and if $d\bar{\Gamma}/dr$ is found from equation (13),

$$w(\mathrm{IV}) = \frac{\Lambda}{8\pi R^2} \tag{15}$$

The downwash at P is then the sum

$$w(\mathrm{I}) + w(\mathrm{II}) + w(\mathrm{III}) + w(\mathrm{IV})$$

It is interesting to note that the three-dimensional problem has been reduced to one of two-dimensional flow, as may be seen by replacing $\bar{\Gamma}$ with its original expression (equation (9)) in equation (11), which may then be written

$$w(0) = \int_0^\infty \frac{-\dfrac{d\int_0^{2\pi}\Gamma\,d\psi}{dr}\,dr}{4\pi(r-0)} \tag{16}$$

Equation (16) is recognized as the usual formula for the induced normal velocity, with the load expressed in the form of a definite integral, and suggests that the first integration (except that the factor $1/2\pi$ was introduced) was equivalent to concentrating all the vorticity around each circle at a single point at the distance r along a line of infinite extension from P. The loaded line of figure 5 may be considered, except for the factor $1/2\pi$, to be the equivalent of the original lifting surface in its effect at P.

EXAMPLES

The method will be applied to check the elliptical distribution of lift conventionally assumed for an uncambered elliptical wing. This distribution, arrived at by combining the two-dimensional theories, does not take account of sweepback or stagger of the lifting elements. In the application of the present method, three cases of elliptical chord distribution will be investigated, two with a straight 50-percent-chord line, and one with the 50-percent-chord line swept back about 30°, the sections remaining parallel to the plane of symmetry. The calculation of the vertical velocities over the sweptback wing will be carried out herein in some detail in order to illustrate the method. The downwash will be found at several points along the three-quarter-chord line. The downwash at the three-quarter-chord point of a section is of particular interest because, from the thin-wing-section theory (reference 6, p. 82), the effective angle of attack of the section is given by the slope of the camber line in the neighborhood of that point, if the camber is approximately circular.

SWEPTBACK WING

For the chordwise lift distribution, the two-dimensional flow around a flat plate as given by the thin-wing-section theory is assumed. This lift distribution and the circulation function obtained by integrating it are shown in figure 6. In

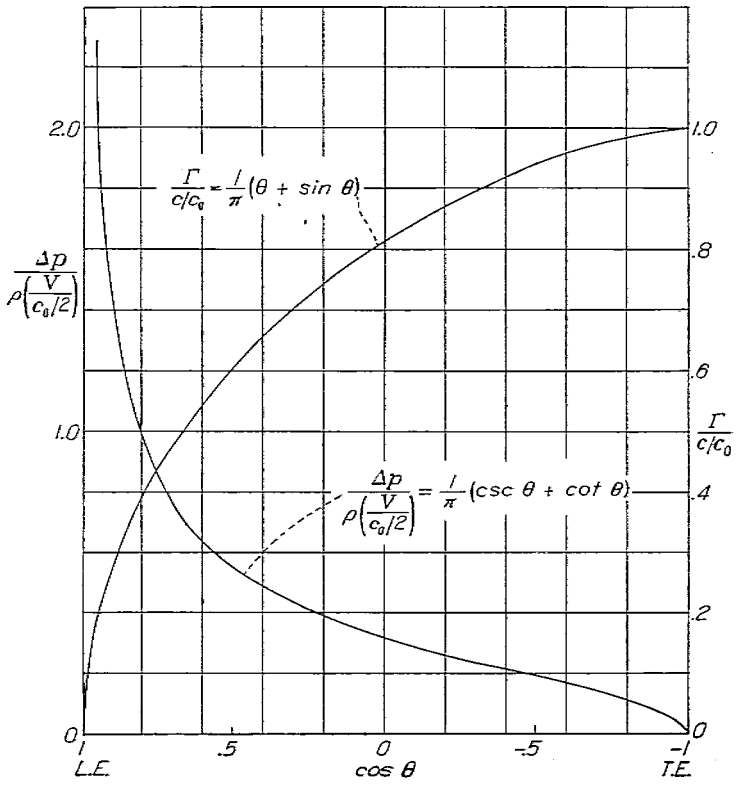

FIGURE 6.—Chordwise pressure distribution and circulation function assumed for figure 7 from the two-dimensional-flow theory for a flat plate.

this case the mathematical expression for the pressure difference is known and Γ can be found analytically. For convenience, the units have been so chosen that the maximum value of Γ is 1.0. If, further, all lengths are expressed in terms of the semispan (measured perpendicular to the plane of symmetry) as the unit of length, the total circulation (Γ at the trailing edge) is simply $\sqrt{1-y^2}$, where y is the distance spanwise from the center line. The resulting contour lines of Γ appear, for the sweptback wing, as in figure 7. The points at which the downwash will be found are also shown.

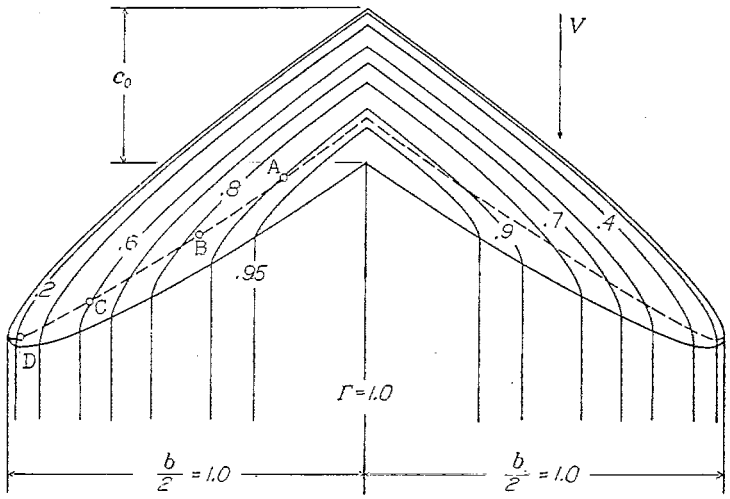

FIGURE 7.—Contour lines of elliptically distributed load over sweptback wing and wake. Aspect ratio, 6.

In order to find the downwash at point B, circles spaced as shown in figure 8 are drawn about this point and the values of Γ indicated by the contour lines intercepted by each circle are plotted against the angular location ψ of the points of intersection. Of the curves for $\Gamma(\psi)$ corresponding to the circles of figure 8, five typical ones are shown in figure 9. The curves designated for $r=0.067$ and $r=0.20$ are characteristic of circles close to the downwash point; the curve for $r=0.216$ includes a point $\left(\frac{\psi}{2\pi}=0.883\right)$ at which the

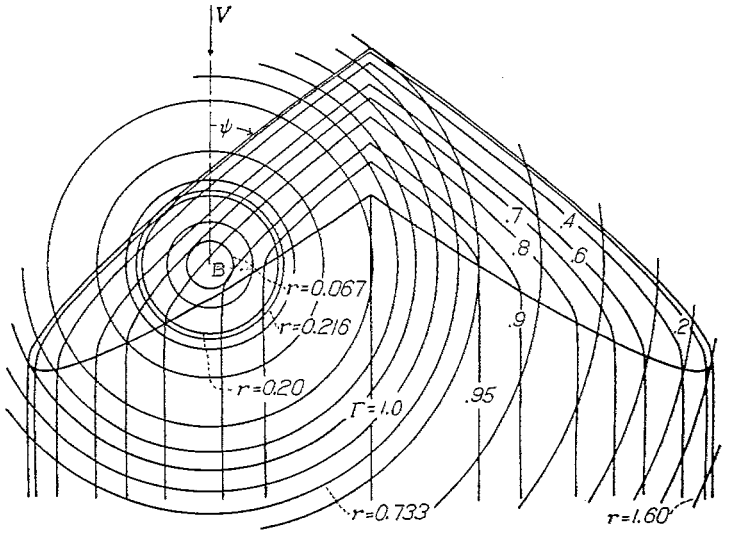

FIGURE 8.—Circles of integration drawn on vortex pattern. The circles corresponding to the curves of figure 9 are identified.

circle is tangent to the leading edge of the wing; the circle of radius 0.733 lies partly ahead of the wing, where $\Gamma=0$, partly on the wing, and partly in the wake; the circle of radius 1.60 traverses the vortex pattern across the wake only.

The results of integrating these curves are plotted against r in figure 10. Since the circulation across the wake is $\sqrt{1-y^2}$, the integral A is $\pi/2$ and the asymptote for the curve of $\bar{\Gamma}(r)$ is, from equation (13), $\bar{\Gamma}=\frac{1}{4r}$. The downwash is now calculated as follows:

It is found that the polynomial

$$\bar{\Gamma}=0.8335-2.70r^2-6.57r^4$$

fits the curve of $\bar{\Gamma}$ through $r=0.20$. Then the downwash contributed by the section from 0 to 0.2 is, from equation (14)

$$w(\mathrm{I})=0.575$$

Section II, with k small, is taken to include both inflection points (there is a third inflection point at 1.78, but its effect is negligible). The following table shows the downwash computations for this section and for the succeeding one:

r	$\bar{\Gamma}$	$\Delta\bar{\Gamma}$	$\frac{\Delta\bar{\Gamma}_{2n}}{r_{2n}}$	$\frac{\Delta\bar{\Gamma}_{2n+1}}{r_{2n}}$
Section II; $k=1.07$				
0.200	0.715	−0.025	−0.125	
.214	.690	−.033		−0.165
.229	.657	−.021	−.092	
.245	.636	−.016		−.070
.262	.620	−.014	−.053	
.280	.606	−.013		−.050
.300	.593	−.011	−.033	
.321	.582	−.013		−.043
.344	.569	−.009	−.026	
.368	.560	−.010		−.029
.393	.550			
Totals:		$w(\mathrm{II})=0.320$	−.329	−.357
Section III; $k=1.20$				
0.393	0.550	−0.026	−0.066	
.472	.524	−.027		−0.069
.566	.497	−.044	−.078	
.679	.453	−.074		−.131
.815	.379	−.062	−.076	
.976	.317	−.049		−.060
1.173	.268	−.049	−.042	
1.408	.219	−.066		−.056
1.790	.153	−.022	−.012	
2.028	.131	−.023		−.013
2.433	.108			
Totals:		$w(\mathrm{III})=0.250$	−.274	−.329

Section III extends to $r=2.433$, where $\bar{\Gamma}=0.108$ and $\frac{1}{4r}=0.103$. The downwash induced by the asymptote from $r=2.433$ out to infinity is only $\frac{1}{16(2.433)^2}$, or 0.011, about 1 percent of the total due to the curve of $\bar{\Gamma}$, and the 5-percent error in the ordinate may therefore be neglected. The total downwash at B is then

$$w(\mathrm{I})+w(\mathrm{II})+w(\mathrm{III})+w(\mathrm{IV})=1.156$$

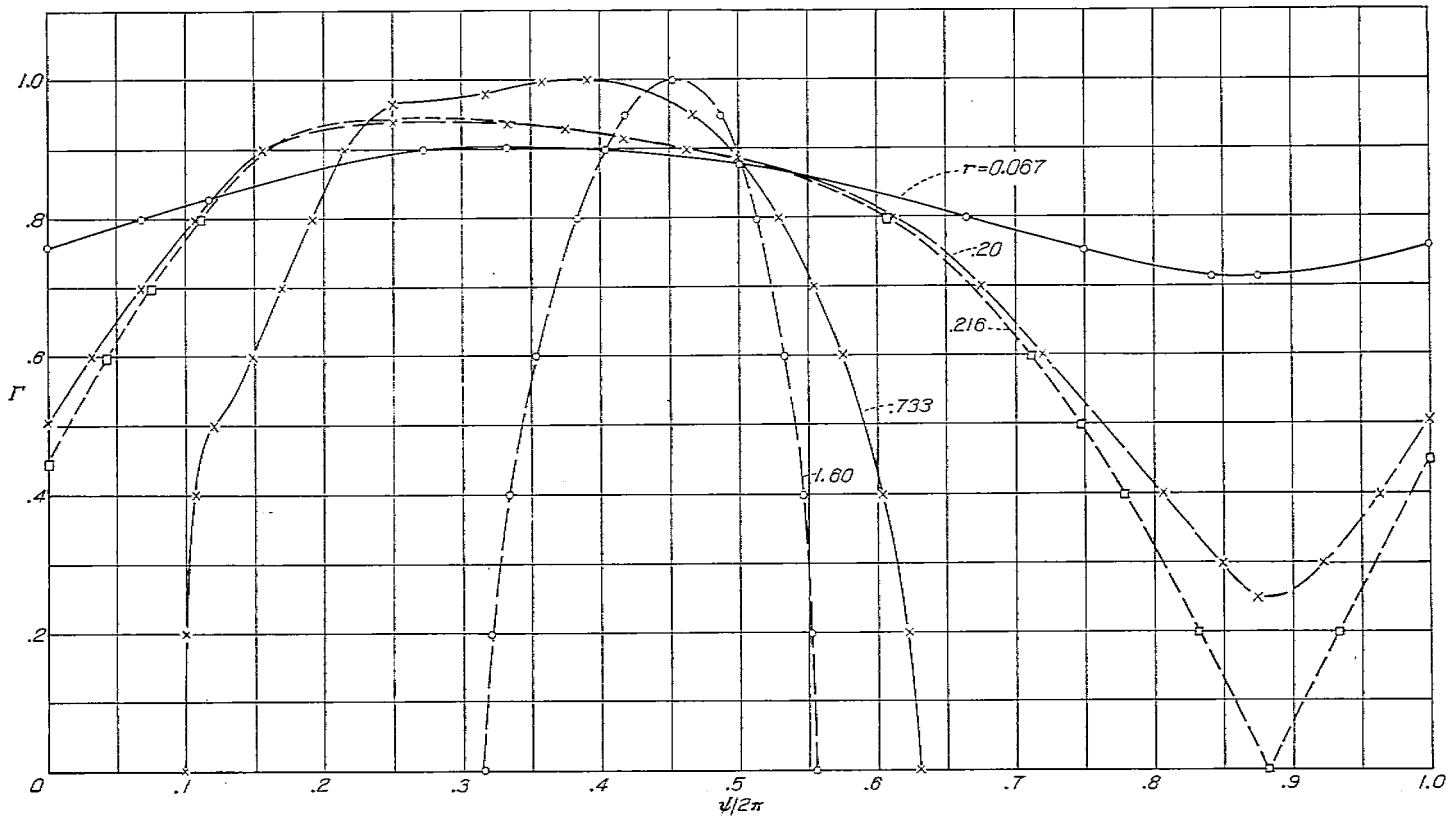

FIGURE 9.—Typical curves for the variation of Γ around a circle. The curves shown correspond to the circles identified in figure 8.

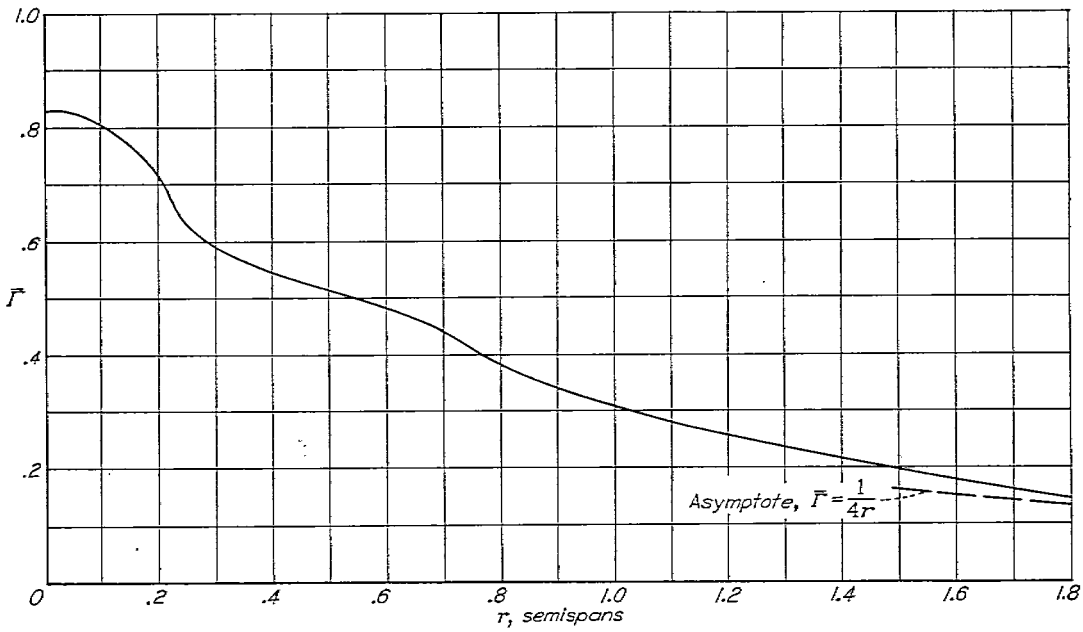

FIGURE 10.—Curve of $\bar{\Gamma}$ (r) for point B of figure 7.

The downwash at points A, C, and D is found in the same way. Figure 11 shows the curves of $\bar{\Gamma}$ for these points. The asymptote $\bar{\Gamma}=\frac{1}{4r}$ is, of course, common to all the curves for this wing.

The downwash is plotted against the spanwise location of the points in figure 12. The quantities Γ_{max} and $b/2$, heretofore assumed to be unity, are included to make the result nondimensional. This curve of the downwash or vertical velocity at the three-quarter-chord line, since the slope of the

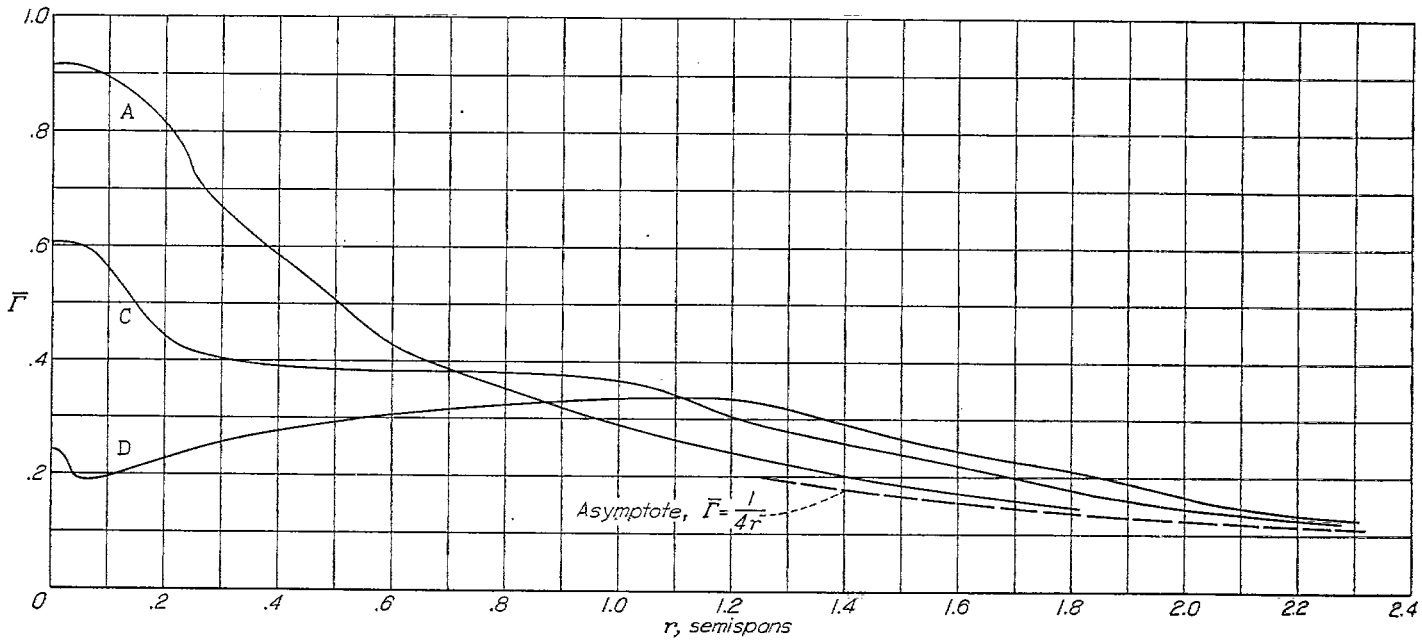

FIGURE 11.—Equivalent loaded lines for points A, C, and D of the sweptback wing of figure 7.

surface is w/V, is a measure of the amount of twist the wing must have to sustain the assumed distribution of lift. If the wing were actually flat, which was the premise in deriving the distribution from the two-dimensional theories, w would be equal to 1.0 all over the surface, so that the deviation of the curve from the line $w=1$ indicates the amount by which the two-dimensional theories are in error when applied to three-dimensional flow. The discontinuity in vorticity at the center line gives rise to a discontinuity in the downwash, which goes to infinity everywhere along the center section. This result indicates that the assumed condition, in which the vortex lines bend to form an angle, cannot exist in practice.

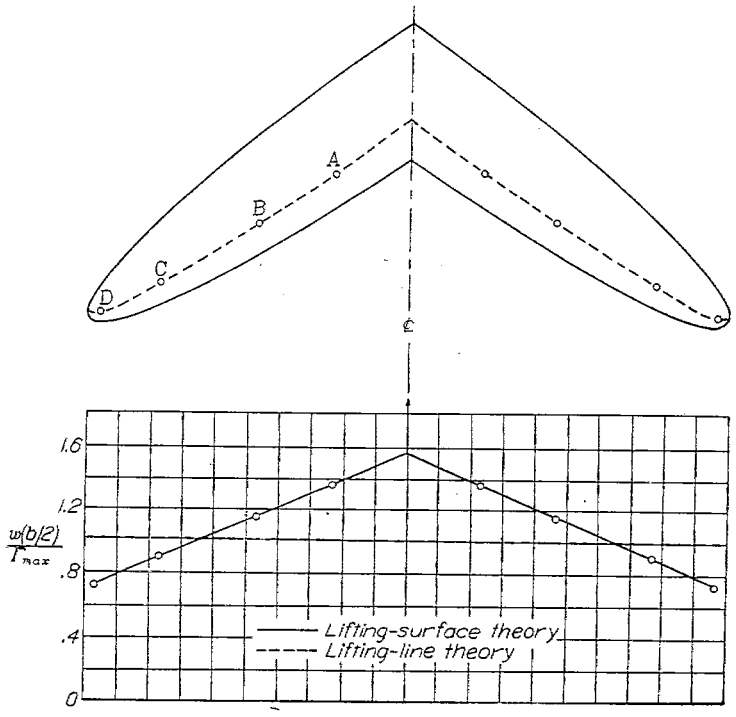

FIGURE 12.—Vertical velocity w at the three-quarter-chord line of the sweptback wing with distribution of load calculated by two-dimensional-flow theories.

UNSWEPT WINGS—ASPECT-RATIO EFFECT

The corresponding curve for the straight elliptical wing of aspect ratio 6 is shown in figure 13. In this case, the downwash was computed also at points along the quarter-chord line. The slope of the surface was found to be less than the slope at the corresponding three-quarter-chord points. The positive camber thus indicated is very small at the center but increases sharply near the tips.

The corresponding curves for the wing of aspect ratio 3 are shown in figure 14. Although the deviation from the lifting-line-theory value is greater, on a percentage basis, than in the case of aspect ratio 6, the agreement with lifting-line theory is still rather good. It may be concluded that, except near the tips, the two-dimensional theories may be considered generally adequate for straight wings.

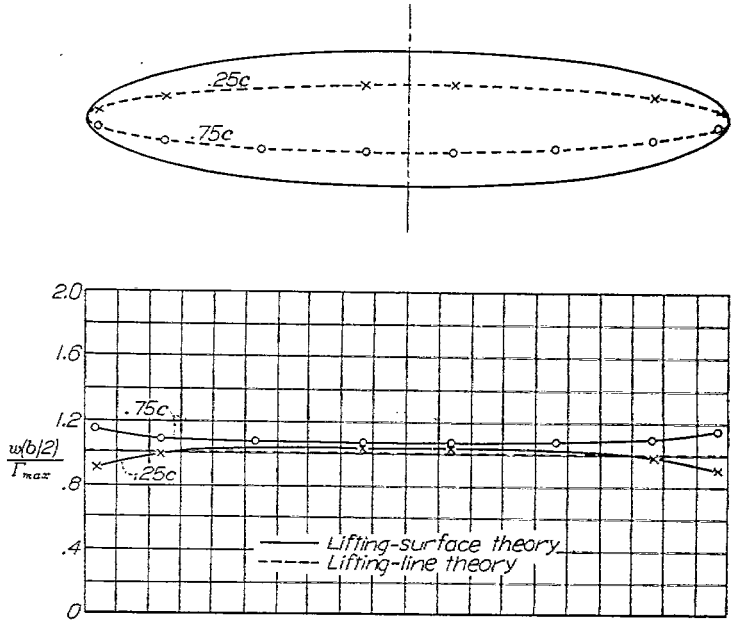

FIGURE 13.—Vertical velocity w at points on straight elliptical wing, aspect ratio of 6, with distribution of load calculated by two-dimensional-flow theories.

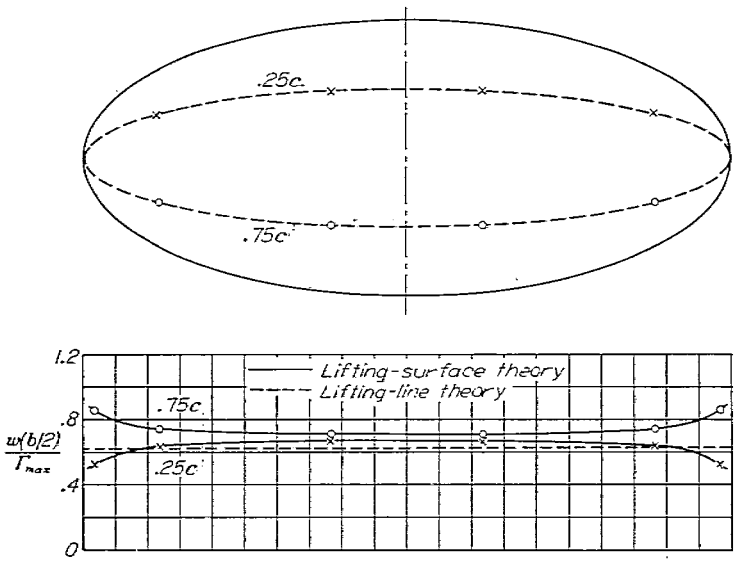

FIGURE 14.—Vertical velocity w at points on straight elliptical wing, aspect ratio of 3, with distribution of load calculated by two dimensional-flow theories.

AN APPLICATION TO THE REVERSE PROBLEM: THE LOAD OVER A FLAT, SWEPTBACK WING

The results of the preceding calculations for the sweptback wing (fig. 12) indicate that for a flat surface the vortex lines over such a wing would actually be rounded off at the center and the load in that region thereby reduced below that of the adjoining sections. It is also apparent that the downwash induced over the tip regions would have to be increased; this would be accomplished by increasing the density of the vortex lines (or lift) toward the tips at the expense of the lift farther inboard.

With these requirements in mind, a second approximation to the lift distribution was assumed; and the downwash at points along the quarter-chord and three-quarter-chord line was found. This approximation proved to be in error in the opposite direction; that is, the downwash now increased from center to tip. A slight modification of this second distribution made the resulting downwash variation linear along the span with, however, a smaller slope than given by the two-dimensional distribution. Values of w for the quarter-chord points fell along a line parallel to that for the three-quarter chord and approximately 8 percent below it, indicating a small amount of camber.

It was assumed that interpolation between the second distribution, as modified, and the first (two-dimensional) approximation, at the same angle of attack, would be a fairly accurate solution to the problem. The curves presented are the result of this interpolation.

Figure 15 shows the final configuration of vortices for the flat sweptback wing. The concentration of lift in any region is proportional to the density of the lines. The entire pattern is independent of angle of attack, except as the basic theory breaks down at large angles of attack.

In figure 16 is shown the span loading. The calculated load is compared with the elliptic load, which has been found to be fairly accurate for the straight wing at an aspect ratio of 6. The induced camber noted in figure 13 for this case is approximately the same, on the average, as remained in the sweptback wing after the last adjustment, so that the wings may be considered comparable.

When the two wings are at the same angle of attack, measured by the slope of the surface at the three-quarter-chord line, the area under the lift curve for the sweptback wing is 86 percent of that under the ellipse, indicating a loss due to sweepback of 14 percent of the total lift. The effect of sweepback on the spanwise variation of lift is indicated by the curve for the straight elliptic wing supporting the same total lift. The effects of sweepback are seen in the higher concentration of load at the wing tips and the depression in the load curve near the center.

USE OF THE METHOD AT WING TIPS

It is expected that the method outlined herein will be especially useful in investigating the nature of the flow near the wing tip, where two-dimensional approximations no longer can be applied. The more accurate three-dimensional treatments available are also unsuitable for this purpose because the calculations fail to converge at the tips. The

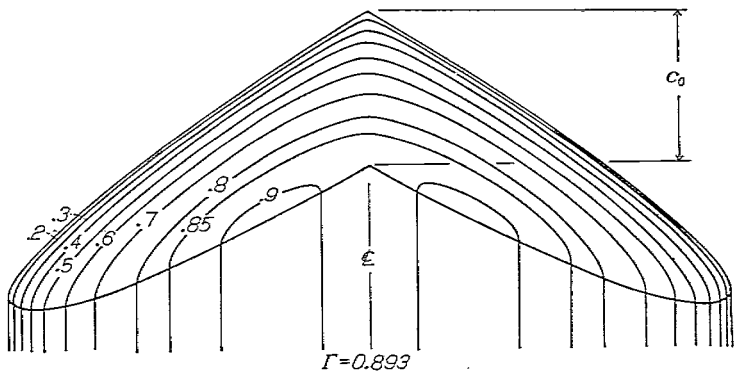

FIGURE 15.—Distribution of vorticity or circulation over flat elliptical wing, aspect ratio of 6, swept back 30°.

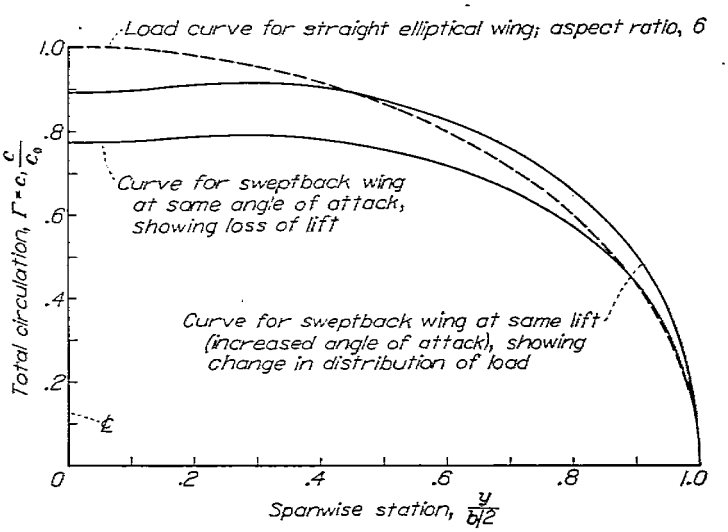

FIGURE 16.—Span-load curves for a wing with elliptical chord distribution, showing the effects of 30° sweepback.

method of calculation described in this paper presents no particular difficulty in these regions. As a test of the accuracy obtainable, the induced downwash was computed at a point near the edge of a circular plate in nonlifting potential and flow was found to check almost exactly with the known solution.

Nevertheless, results obtained for the tips have qualitative rather than quantitative value (except for low angles of attack). The validity of the theory is actually limited by the existence of strong tip vortices, which may cause the vortex sheet to curl up out of the plane in which it is assumed to lie. On the other hand, the high concentration of vorticity associated with this effect adds appreciably to the drag of the wing, so that even a general indication of such a concentration of load at the tips is of value. It should be possible to design, by the use of the present method, a wing tip that would avoid this effect by providing a fairly gradual tapering off of the load spanwise. At the same time, a favorable chordwise gradient could be specified. Thus, it appears likely that an optimum tip for low drag could be deduced.

LANGLEY MEMORIAL AERONAUTICAL LABORATORY,
NATIONAL ADVISORY COMMITTEE FOR AERONAUTICS,
LANGLEY FIELD, VA., *May 16, 1942.*

REFERENCES

1. Prandtl, L.: Recent Work on Airfoil Theory. NACA TM No. 962, 1940.
2. Kinner, W.: Die kreisförmige Tragfläche auf potential-theoretischer Grundlage. Ing.-Archiv, Bd. VIII, Heft 1, Feb. 1937, pp. 47–80.
3. Krienes, Klaus: The Elliptic Wing Based on the Potential Theory. NACA TM No. 971, 1941.
4. Glauert, H.: The Elements of Aerofoil and Airscrew Theory. Cambridge Univ. Press, 1930.
5. Von Kármán, Th., and Burgers, J. M.: General Aerodynamic Theory—Perfect Fluids. Vol. II of Aerodynamic Theory, div. E, W. F. Durand, ed., Julius Springer (Berlin), 1935.
6. Munk, Max M.: Fundamentals of Fluid Dynamics for Aircraft Designers. The Ronald Press Co., 1929.